

# Visualizing Uncertainties in Ensemble Wildfire Forecast Simulations

Jixian Li\*

Timbwaoga A. J. Ouermi†

Chris R. Johnson‡

Scientific Computing and Imaging Institute, University of Utah

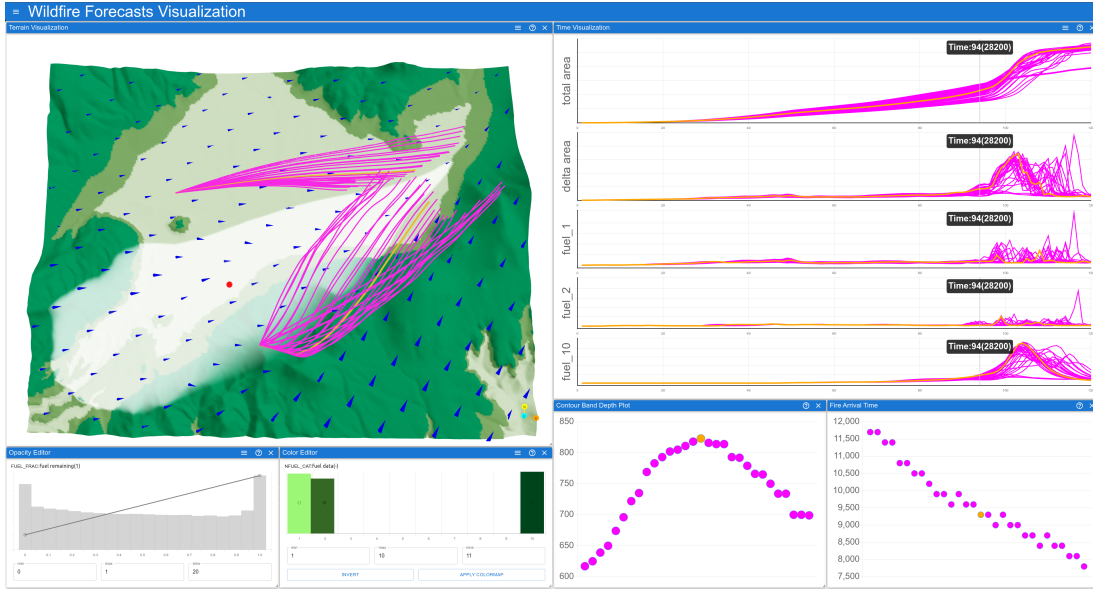


Figure 1: An overview of the ensemble wildfire visualization interface. Our interface supports transfer-function-based color and opacity mapping for visualizing scalar functions from wildfire simulations, glyph- and streamline-based wind visualization, temporal events summary, contour band depths, spatial query for the fire arrival time (red sphere in the terrain shows the query point).

## ABSTRACT

Wildfires pose substantial risks to our health, environment, and economy. Studying wildfires is challenging due to their complex interaction with the atmosphere dynamics and the terrain. Researchers have employed ensemble simulations to study the relationship among variables and mitigate uncertainties in unpredictable initial conditions. However, many wildfire researchers are unaware of the advanced visualization available for conveying uncertainty. We designed and implemented an interactive visualization system for studying the uncertainties of fire spread patterns utilizing band-depth-based order statistics and contour boxplots. We also augment the visualization system with the summary of changes in the burned area and fuel content to help scientists identify interesting temporal events. In this paper, we demonstrate how our system can support wildfire experts in studying fire spread patterns, identifying outlier simulations, and navigating to interesting times based on a summary of events.

**Index Terms:** Ensemble Visualization, Uncertainty Visualization, Wildland Fire

## 1 INTRODUCTION

Wildfires in the western United States cause significant damage to ecosystems, properties, and quality of life, which has resulted in substantial economic losses [8, 31, 15], and the frequency and the area burned by these wildfires are predicted to increase. To effectively manage resources and assess the risk of wildfires, domain scientists have been using simulations to study wildfire behavior and its socioeconomic impact [16, 10]. In the real world, unforeseeable conditions, such as sudden shifts in wind patterns or changes in fuel moisture content, may drastically impact how fire propagates. To better understand and mitigate the risks from unknown conditions, scientists study the spread pattern of fire from a collection of initial conditions and different parameter values [1, 2, 4, 23].

We have collaborated with wildfire and simulation experts to understand their workflows and explore how visualization could help them achieve their goals. In their workflows, they use simulation tools such as WRF-SFIRE [19] or QES-FIRE [22] to simulate fire progression over time. One of the most important outcomes of their simulations is the location of the fire front. Fires have different spreading rates depending on the fuel, terrain, and wind at the fire front. Thus, we observe different spread patterns depending on how the simulation is set up. The fire propagation pattern is especially complex when the fire interacts with the atmosphere, including wind and heat exchange [20].

Even though our collaborators utilize ensemble methods in their analysis to mitigate the uncertainty observed in weather and fuel content, they apply limited uncertainty visualization techniques. We have noticed that they are not alone. Few uncertainty visualization techniques have been applied in existing ensemble wildfire simulation research. Hullman [11] has looked into the challenges of

\*e-mail:jixianli@sci.utah.edu

†e-mail:touermi@sci.utah.edu

‡e-mail:crj@sci.utah.edu

including uncertainties in visualization. Despite the challenges, we have seen some attempts to convey uncertainty in ensemble wildfire visualizations. In some probabilistic fire models, researchers plot a map indicating the probability of the spatial location being burned [1, 24, 6]. Those maps are provided alongside a deterministic model or observed data to provide the context of the fire front. However, the geometry of the fire front of the ensemble members is lost in the probabilistic modeling. We also have observed significant usage of small multiples and spaghetti plots for studying ensembles [29, 6].

Since uncertainty quantification and visualization has been identified as one of the top problems in scientific data visualization [13, 14], many visualization techniques on uncertainty have been explored and studied [3, 9, 25]. For ensemble data, researchers have been exploring visualization techniques to efficiently analyze information buried within multiple instances of spatial-temporal and often multivariate data [26, 5].

One particular line of research focuses on extracting meaningful and robust statistics for complex data such as fire front contours. Extending the definition of functional band depth [17] to geometric shapes such as contours, curves, and surfaces [28, 21, 7], researchers have developed robust statistics for nonparametric distributions that preserve the global structures of the geometries. The visualizations of the statistics reduce the visual clutter when plotting every instance of ensemble members while highlighting the most representative trends and variations.

To introduce uncertainty visualization techniques to wildfire scientists, we have created an interactive visualization system that incorporates contour boxplot-based visualization. Our system summarizes the trends and variations in the contours to help researchers better understand fire propagation sensitivity in different experimental parameters. Utilizing the contour band depths can also help scientists identify anomalies and outliers in the simulations. To assist the study of the time-varying data, we added change-over-time curves to help users identify events and navigate between different simulation instances. Our interface also allows users to specify a spatial region and visualize the distribution of fire arrival time. This feature is particularly useful when a wildfire researcher has a region of interest, such as an observation tower, in the simulated domain.

The contribution of this paper is a new visualization tool with an interactive interface to study spread patterns from wildfire ensemble simulations. We showcase how uncertainty visualization techniques can help wildfire experts quickly identify patterns and outliers in wildfire simulations.

## 2 ENSEMBLE WILDFIRE VISUALIZATION

We designed our interface around the wildfire forecast simulation WRF-SFIRE [19]. Our data assumes that the ensemble members have the same spatial description; that is, there is no uncertainty in the topographic characteristics of the terrain. The sampling grid is shared among all ensemble members. Other parameters, such as fuel content, fire spread, or wind vectors, can vary among simulations. To visualize an ensemble of time-varying fires, our interface design is split into two major components: Visualization of a single time and visualization of a temporal events summary to guide users in selecting the time. For single-time visualization, we developed multiple ensemble visualization techniques to summarize the differences between ensemble members. We provide a temporal overview and spatial query for the temporal events to help users select the time they want to look at.

### 2.1 Visualizing Uncertainty in Fire Spread Pattern

For ensemble wildfire simulations, one of the most important questions researchers ask is how the wildfire spreads differently in different simulation settings. For example, researchers can perturb the initial wind velocity or fuel moisture to simulate uncertain weather

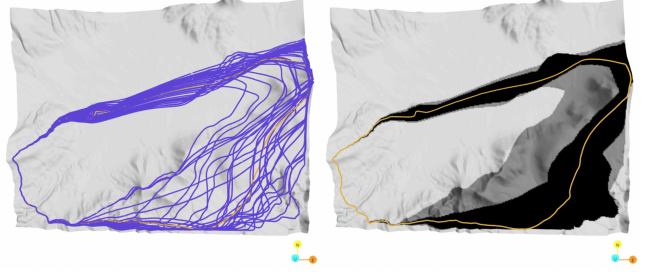


Figure 2: Ensemble contour visualization. On the left, we plot every instance of fire contours. On the right, we plot the contour boxplot as the summary to reduce visual clutter.

conditions and see how the fire propagates under different initial conditions.

We visualize the fire propagation by tracking the location of the fire front contour. For level set methods-based simulation tools, such as WRF-SFIRE, the fire front is the 0-level set of the level set function [18]. We can extract the isocontour from each simulated instance. To visualize the ensemble simulations, a simple and naive approach is to plot all the contours together. Figure 2 shows an example of this visualization on the left.

This type of visualization has some drawbacks. For example, in the region where the separation between each simulation is low, multiple contours are plotted at the same location. Therefore, the simulations are not distinguishable. Similarly, this visualization suffers from the same problem in regions with many crossings between contours. We utilize the contour boxplot [28] to build a visual summary of the spread of contours. As shown in the right image of Figure 2, the orange contour is the median. The black and darker gray regions contain the center-most 50% and 90% of the contours from all simulations, respectively. Compared to the image on the left, this visualization reduces visual clutter in the region where contours cross each other and highlights the median contour.

The contour boxplot computations extend the definition of functional band depths [27]. For a scalar field  $f : X \rightarrow \mathbb{R}$ , an isocontour of value  $v$  is the level set  $L_f = \{x | f(x) = v\}$ . The area enclosed by the isocontour is the sublevel set  $L_f^- = \{x | f(x) < v\}$ . A band formed by a set of contours is defined as the intersection of the sublevel sets subtracted from the union of the sublevel sets. Assume a set of scalar function  $S = \{f_1, f_2, \dots, f_n\}$ ,

$$\text{band}(S) = \{L_{f_1}^- \cup L_{f_2}^- \cup \dots \cup L_{f_n}^-\} - \{L_{f_1}^- \cap L_{f_2}^- \cap \dots \cap L_{f_n}^-\} \quad (1)$$

Then, the contour band depth of a contour  $L_{f_i}$  is the number of bands this contour lives fully inside, considering the bands formed by all subsets of the ensemble  $E$

$$\text{depth}(i) = \sum_{S \subseteq E} \mathcal{I}(L_{f_i}, \text{band}(S)) \quad (2)$$

where  $\mathcal{I}$  is an indicator function that is 1 when  $L_{f_i}$  is fully contained in the band, 0 otherwise. Sometimes the band depth is normalized to a probability by adding a scale term. In the computation, the loop over all subsets is  $O(2^n)$  for an  $n$ -member ensemble, which creates a performance bottleneck. López-Pintado and Romo [17] have established that using only 2-element subsets is often sufficient to arrive at stable statistics. Therefore, we consider only bands formed by two contours in the band depth computation, which reduces the number of loops for each contour to  $O(n^2)$ . For each contour, we can compute the band depth. Sorting all the contours by their band depths gives us a center-outwards ordering of all the contours. The contour with the most depth is then the median. We can derive similar notions of quantiles for contours according to this ordering.

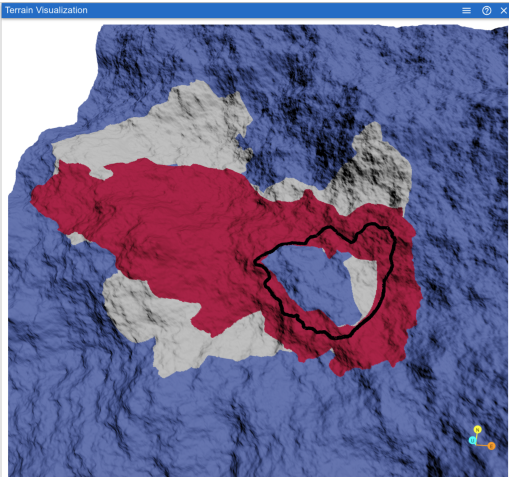


Figure 3: Demonstration of the contour boxplot on randomly generated terrain with varying northwest wind. The black contour is the median contour. The red region encloses 50 percent contours ordered by contour band depths. The gray region encloses 90 percent of all contours, which we consider the nonoutliers.

Throughout our study, the domain resolution is between  $200^2$  and  $500^2$ . The number of ensemble members is 31. Computing the contour band depths for 31 instances of a  $512^2$  grid takes 5.8 seconds on a single core of an AMD EPYC 7542 processor. With CuPy<sup>1</sup> acceleration, the computation times are reduced to 0.7 seconds on an NVIDIA A100 GPU. Our implementation can fit at least 200 instances of a  $512^2$  grid into the GPU memory. The time it takes to compute 200 contours with a  $512^2$  terrain is 1 minute 6 seconds on a GPU and 28 minutes on a sequential CPU. The computation cost increases cubically with an increase in the number of ensembles and increases linearly with the resolution of the sampling grid. Therefore, our implementation supports the interactive computation of contour band depth for our data resolution ( $31 \times 512 \times 512$  for each temporal slice) with some room to support larger scale or more ensemble members.

To demonstrate how contour boxplots can help wildfire researchers analyze the data, we created a randomly generated domain with southeast winds at 31 initial velocities from 1 to 2 m/s. The contour boxplot shows some interesting features in the Figure 3. First, the distribution of the contours is asymmetric. Contours outside the median cover a much larger area than those inside, especially in the initial wind direction. We then examined individual instances and found that the spread is much larger in simulations with higher initial wind velocities, which suggests fire propagation is more sensitive to higher wind velocity. Also, the plot has some large gray regions. We noticed that those gray regions are normally associated with a high-positive terrain slope. This finding confirms our collaborators' hypothesis that fire climbs faster than traveling on plain ground.

Contour band depth can also help researchers detect outliers. The definition of an outlier depends on the data and domain knowledge. However, contour band depths can help us understand how the contours overlap. A lower band depth means the contour is more likely to differ from other ensemble members. We plot the contour band depths value as a scatter plot. The x-axis is the experiment ID, and the y-axis is the contour band depths. Figure 4 shows a set of simulations where some experiments contain numerical instability. The contour boxplot uses black and dark gray to indicate center-most 50% and 90% contours, respectively. The orange contour has a long tail in the north direction outside areas covered by 90% of contours. This means the fire front of the selected simu-

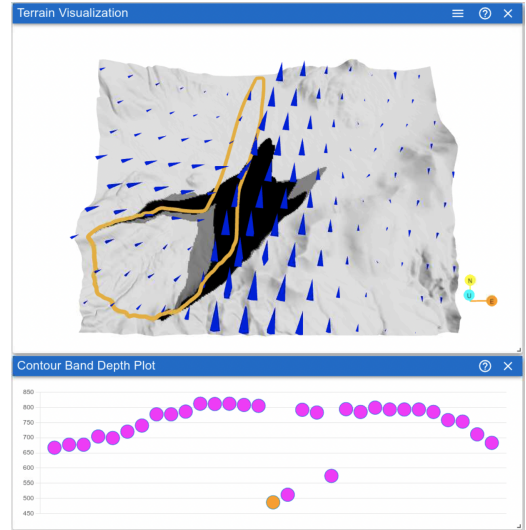


Figure 4: An example of an outlier of the simulations. The orange dot in the contour band depth plot is the currently selected member shown in the terrain visualization. A lower contour band depth value indicates a higher possibility of the ensemble member being an outlier.



(a) Google map of the simulated area. (b) Three types of fuel are placed over the domain according to the elevation.  
Figure 5: Our simulation domain. We simulated 31 instances of fire in 8km  $\times$  6km area of Valles Caldera, New Mexico, USA

lation is stretched north in contrast to most simulations. The wind glyph helps us identify a large band of high-magnitude south wind in the center of the simulation domain caused by numeric issues.

In addition to the contour boxplot, we implemented standard scalar and vector field visualization tools to visualize individual simulations at a selected time point. We employed the opacity and transfer functions mapping to map a user-chosen scalar field to visual encodings of the terrain. Our interface allows users to edit the piecewise-linear opacity and color transfer functions to edit the visual encodings. We also provide glyph-based and streamline-based surface wind visualization as demonstrated in Figure 1.

## 2.2 Visualizing Evolution of Wildfire

Wildfires are time-varying by nature. How different simulations evolve differently is an important aspect of ensemble analysis. An overview of fire propagation along the temporal axis helps researchers identify significant events. This overview can guide researchers to select interesting points in time and study fire propagation using previously mentioned tools.

Our temporal overview focuses on the magnitude of changes, particularly how burned areas change. A significant change in the burned area indicates a shift in the fire-spreading pattern, which could result from a shift in wind pattern, terrain slope, or fuel content.

To summarize changes, we sum the amount of burned area over the spatial domain for each time and report the difference between the current timestamp and the previous timestamp. In addition to

<sup>1</sup><https://cupy.dev/>

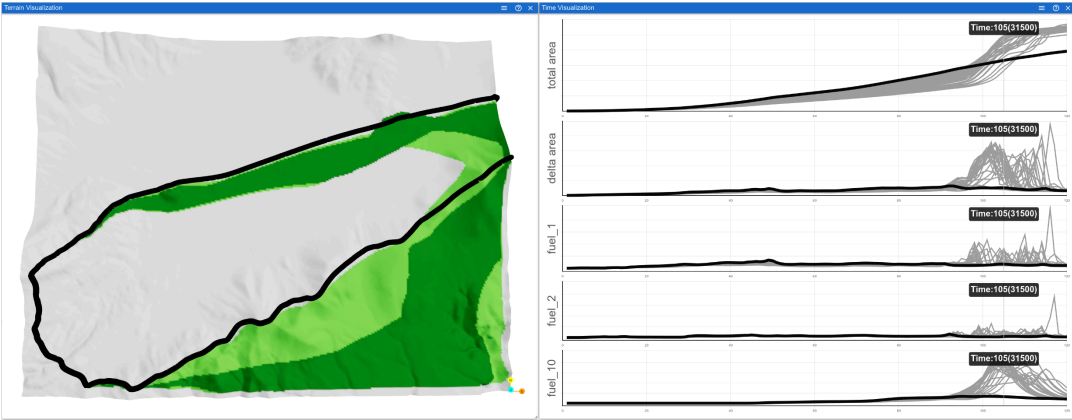


Figure 6: Demonstration of the temporal overview visualization. On the right, we summarize the magnitude of changes in the burned area and different fuel types. Most of the simulations have increased the burning of **fuel.10** after the 100th timestamp. We observed three instances without significant changes in the amount of **fuel.10** burned. On the left, we plot one of the instances in the context of the contour boxplot. This particular instance does not reach the southeast portion of the domain where most other firefront contours reside at the 105th timestamp.

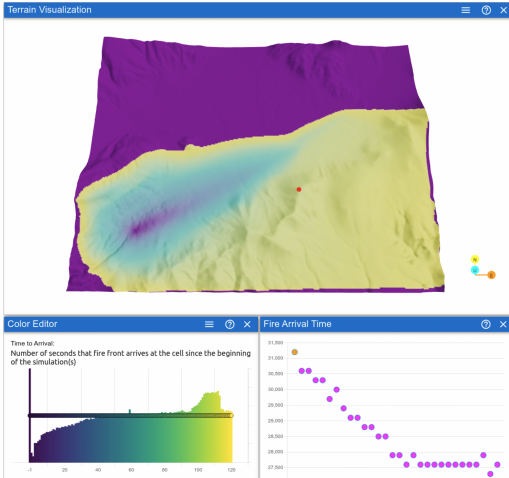


Figure 7: This plot uses the viridis colormap to show the time when the firefront arrives. Our interface also allows users to select a point (red dot) in the domain and visualize the distribution of arrival time for all ensemble members (bottom right).

the changes in the fire area, we also report changes in the fuel by different fuel types. We plot individual change over time curves and let users highlight each instance by hovering and clicking the mouse. Therefore, we did not employ summary statistics for the curves.

**Figure 6** shows an example of identifying a specific temporal pattern using our interface. The dataset is simulated over an 8km × 6km area of Valles Caldera, New Mexico, USA, which is the site of two recent fires: Las Conchas (2011) and Thompson Ridge (2013). The simulation grid resolution is 345 × 265 with 120 steps in time. The temporal step size is 300 seconds. The simulated wind is linearly sampled with an initial magnitude from 4 to 7 m/s with 31 samples. The x and y components of the wind velocity are divided in a 5:1 ratio toward the east-northeast direction. Three types of fuel content are placed by the terrain’s altitude. **fuel.1**, **fuel.2**, and **fuel.10** are short grass, timber (grass and understory), and timber (litter and understory), respectively. **Figure 5** shows our simulated domain.

The change over time curves in the **Figure 6** shows most of the simulations follow a pattern that fire gradually grows before the 90th timestamp. Around that time, most of the fire contours start growing toward the large region of **fuel.10** in the southeast mountain. However, we observe three instances of simulations without

significant changes in **fuel.10**. Selecting them from the time visualization by clicking their curves, we notice that these instances are the simulations with the three largest initial wind velocities. Because the wind velocity magnitude is so high, the wind dominates how fire grows in those simulations. We can see a long and thin burned area aligned with the initial wind direction for each instance compared to the contour boxplot shown for other instances of the simulations.

In addition to the temporal event, our collaborators requested visualization of the spatial event. Given a point in space, they want to know when the fire arrives. We implemented two visualizations for this task. For a single instance, we report the arrival time as a scalar field so that users can choose color or opacity mapping. Alternatively, users can select a point in the domain, and we use a scatterplot to report the arrival time distribution of all ensemble members for the selected point. **Figure 7** shows an example of spatial event visualization.

### 3 DISCUSSION

This work presented an interactive visualization system that provides wildfire experts with additional visualization techniques for uncertainties in fire propagation. We showcased how the contour band depths and boxplot can efficiently summarize a collection of wildfire ensemble simulations. These techniques help depict the sensitivity of fire propagation and identify anomalies in the simulations. Temporal and spatial events help scientists answer questions about when and where the events happen in the simulation.

Our wildfire simulation collaborators gave us positive feedback on the visualization system, and the interactive interface inspired them to ask questions about different types of uncertainty. For example, one of the challenges of running a simulation is that it takes a long time to run on a high-resolution grid. Therefore, how does changing to a smaller simulation resolution affect uncertainty if the simulation experts want to run simulations on different domain resolutions? Studying uncertainties from different sampling grids requires spatial alignment, which may introduce more types of uncertainty, such as interpolation errors. We aim to address different types of uncertainty in the future.

Furthermore, visualization of summary statistics, such as boxplots, is not the only way to visualize distributions. For example, hypothetical outcome plots have been introduced as an effective way of visualizing distributions [12, 30]. We want to examine how well such methods work on geospatial data and establish a formal way to evaluate wildfire uncertainty visualization methods.

## ACKNOWLEDGMENTS

This work was partially supported by the Intel OneAPI CoE, the Intel Graphics and Visualization Institutes of XeLLENCE, and the DOE Ab-initio Visualization for Innovative Science (AIVIS) grant 2428225. We thank Zachary Morrow from Sandia National Laboratory and Matthew Moody from the University of Utah for providing wildfire simulation data.

## REFERENCES

- [1] F. Allaire, J.-B. Filippi, and V. Mallet. Generation and evaluation of an ensemble of wildland fire simulations. *International Journal of Wildland Fire*, 29(2):160–173, 2020. doi: 10.1071/WF19073 1 2
- [2] A. Benali, A. R. Ervilha, A. C. Sá, P. M. Fernandes, R. M. Pinto, R. M. Trigo, and J. M. Pereira. Deciphering the impact of uncertainty on the accuracy of large wildfire spread simulations. *Science of The Total Environment*, 569–570:73–85, 2016. doi: 10.1016/j.scitotenv.2016.06.112 1
- [3] G.-P. Bonneau, H.-C. Hege, C. R. Johnson, M. M. Oliveira, K. Potter, P. Rheingans, and T. Schultz. *Overview and State-of-the-Art of Uncertainty Visualization*, pp. 3–27. Springer London, London, 2014. doi: 10.1007/978-1-4471-6497-5\_1 2
- [4] M. Cruz. Monte carlo-based ensemble method for prediction of grassland fire spread. *International Journal of Wildland Fire*, 19:521–530, 07 2010. doi: 10.1071/WF08195 1
- [5] C. de Souza, S. Bonnet, D. de Oliveira, M. Cataldi, F. Miranda, and M. Lage. Prowis: A visual approach for building, managing, and analyzing weather simulation ensembles at runtime. *IEEE Transactions on Visualization and Computer Graphics*, 30(01):738–747, jan 2024. doi: 10.1109/TVCG.2023.3326514 2
- [6] M. A. Finney, I. C. Grenfell, C. W. McHugh, R. C. Seli, D. Trethewey, R. D. Stratton, and S. Brittain. A method for ensemble wildland fire simulation. *Environmental Modeling and Assessment*, 16(2):153–167, Nov. 2010. doi: 10.1007/s10666-010-9241-3 2
- [7] M. G. Genton, C. Johnson, K. Potter, G. Stenchikov, and Y. Sun. Surface boxplots. *Stat*, 3(1):1–11, 2014. doi: 10.1002/sta4.39 2
- [8] D. F. Gomez Isaza, R. L. Cramp, and C. E. Franklin. Fire and rain: A systematic review of the impacts of wildfire and associated runoff on aquatic fauna. *Global Change Biology*, 28(8):2578–2595, 2022. doi: 10.1111/gcb.16088 1
- [9] C. D. Hansen, M. Chen, C. R. Johnson, A. E. Kaufman, and H. Hagen. *Scientific Visualization: Uncertainty, Multifield, Biomedical, and Scalable Visualization*. Springer Publishing Company, Incorporated, 2014. 2
- [10] V. Herr, A. K. Kochanski, V. V. Miller, R. McCrea, D. O’Brien, and J. Mandel. A method for estimating the socioeconomic impact of earth observations in wildland fire suppression decisions. *International Journal of Wildland Fire*, 29(3):282–293, 2020. doi: 10.1071/WF18237 1
- [11] J. Hullman. Why authors don’t visualize uncertainty. *IEEE Transactions on Visualization and Computer Graphics*, 26(1):130–139, 2020. doi: 10.1109/TVCG.2019.2934287 1
- [12] J. Hullman, P. Resnick, and E. Adar. Hypothetical outcome plots outperform error bars and violin plots for inferences about reliability of variable ordering. *PLOS ONE*, 10(11), 2015. doi: 10.1371/journal.pone.0142444 4
- [13] C. Johnson. Top scientific visualization research problems. *IEEE Computer Graphics and Applications*, 24(4):13–17, 2004. doi: 10.1109/MCG.2004.20 2
- [14] C. Johnson and A. Sanderson. A next step: Visualizing errors and uncertainty. *IEEE Computer Graphics and Applications*, 23(5):6–10, 2003. doi: 10.1109/MCG.2003.1231171 2
- [15] Y. P. Liao and C. Kousky. The fiscal impacts of wildfires on California municipalities. *Journal of the Association of Environmental and Resource Economists*, 9(3):455–493, 2022. doi: 10.1086/717492 1
- [16] Y. Liu, A. Kochanski, K. R. Baker, W. Mell, R. Linn, R. Paugam, J. Mandel, A. Fournier, M. A. Jenkins, S. Goodrick, G. Achtemeier, F. Zhao, R. Ottmar, N. H. F. French, N. Larkin, T. Brown, A. Hudak, M. Dickinson, B. Potter, C. Clements, S. Urbanski, S. Prichard, A. Watts, and D. McNamara. Fire behavior and smoke modeling: Model improvement and measurement needs for next-generation smoke research and forecasting systems. *International Journal of Wildland Fire*, 28(8):570–588, 2019. doi: 10.1071/WF18204 1
- [17] S. López-Pintado and J. Romo. On the concept of depth for functional data. *Journal of the American Statistical Association*, 104(486):718–734, 2009. doi: 10.1198/jasa.2009.0108 2
- [18] V. Mallet, D. Keyes, and F. Fendell. Modeling wildland fire propagation with level set methods. *Computers and Mathematics with Applications*, 57(7):1089–1101, Apr. 2009. doi: 10.1016/j.camwa.2008.10.089 2
- [19] J. Mandel, S. Amram, J. D. Beezley, G. Kelman, A. K. Kochanski, V. Y. Kondratenko, B. H. Lynn, B. Regev, and M. Vejmelka. Recent advances and applications of WRF-SFIRE. *Natural Hazards and Earth System Sciences*, 14(10):2829–2845, 2014. doi: 10.5194/nhess-14-2829-2014 1, 2
- [20] J. Mandel, J. D. Beezley, and A. K. Kochanski. Coupled atmosphere-wildland fire modeling with wrf 3.3 and sfire 2011. *Geoscientific Model Development*, 4(3):591–610, 2011. doi: 10.5194/gmd-4-591-2011 1
- [21] M. Mirzargar, R. T. Whitaker, and R. M. Kirby. Curve boxplot: Generalization of boxplot for ensembles of curves. *IEEE Transactions on Visualization and Computer Graphics*, 20(12):2654–2663, 2014. doi: 10.1109/TVCG.2014.2346455 2
- [22] M. J. Moody, J. A. Gibbs, S. Krueger, D. Mallia, E. R. Pardyjak, A. K. Kochanski, B. N. Bailey, and R. Stoll. Qes-fire: a dynamically coupled fast-response wildfire model. *International Journal of Wildland Fire*, 31(3):306–325, 2022. doi: 10.1071/WF21057 1
- [23] T. Penman, D. Ababei, J. Cawson, B. Cirulis, T. Duff, W. Swedosh, and J. Hilton. Effect of weather forecast errors on fire growth model projections. *International Journal of Wildland Fire*, 29, 01 2020. doi: 10.1071/WF19199 1
- [24] R. M. Pinto, A. Benali, A. C. L. Sá, P. M. Fernandes, P. M. M. Soares, R. M. Cardoso, R. M. Trigo, and J. M. C. Pereira. Probabilistic fire spread forecast as a management tool in an operational setting. *SpringerPlus*, 5(1):1205, Jul 2016. doi: 10.1186/s40064-016-2842-9 2
- [25] K. Potter, P. Rosen, and C. R. Johnson. From quantification to visualization: A taxonomy of uncertainty visualization approaches. In A. M. Dienstfrey and R. F. Boisvert, eds., *Uncertainty Quantification in Scientific Computing*, pp. 226–249. Springer Berlin Heidelberg, Berlin, Heidelberg, 2012. 2
- [26] K. Potter, A. Wilson, P.-T. Bremer, D. Williams, C. Doutriaux, V. Pasucci, and C. R. Johnson. Ensemble-vis: A framework for the statistical visualization of ensemble data. In *2009 IEEE International Conference on Data Mining Workshops*, pp. 233–240, 2009. doi: 10.1109/ICDMW.2009.55 2
- [27] Y. Sun and M. G. Genton. Functional boxplots. *Journal of Computational and Graphical Statistics*, 20(2):316–334, 2011. doi: 10.1198/jcgs.2011.09224 2
- [28] R. T. Whitaker, M. Mirzargar, and R. M. Kirby. Contour boxplots: A method for characterizing uncertainty in feature sets from simulation ensembles. *IEEE Transactions on Visualization and Computer Graphics*, 19(12):2713–2722, 2013. doi: 10.1109/TVCG.2013.143 2
- [29] World Meteorological Organization. *Guidelines on Ensemble Prediction Systems and Forecasting*. World Meteorological Organization, 2012. available online at [https://library.wmo.int/viewer/48473/download?file=wmo\\_1091\\_en.pdf](https://library.wmo.int/viewer/48473/download?file=wmo_1091_en.pdf) (accessed Jun 2024). 2
- [30] D. Zhang, E. Adar, and J. Hullman. Visualizing uncertainty in probabilistic graphs with network hypothetical outcome plots (nethops). *IEEE Transactions on Visualization and Computer Graphics*, 28(1):443–453, 2022. doi: 10.1109/TVCG.2021.3114679 4
- [31] Y. Zhang, J. Fan, M. Shrivastava, C. R. Homeyer, Y. Wang, and J. H. Seinfeld. Notable impact of wildfires in the western united states on weather hazards in the central united states. *Proceedings of the National Academy of Sciences*, 119(44):e2207329119, 2022. doi: 10.1073/pnas.2207329119 1